HOKKAIDO UNIVERSITY

Title	Brittle-ductile transition of double network hydrogels : Mechanical balance of two networks as the key factor
Author(s)	Ahmed, Saika; Nakajima, Tasuku; Kurokawa, Takayuki et al.
Citation	Polymer, 55(3), 914-923 https://doi.org/10.1016/j.polymer.2013.12.066
Issue Date	2014-02-12
Doc URL	https://hdl.handle.net/2115/55147
Type	journal article
File Information	Manuscript_final.pdf

Hokkaido University Collection of Scholarly and Academic Papers : HUSCAP

Brittle-Ductile Transition of Double Network Hydrogels: Mechanical Balance of Two Networks as the Key Factor

Saika Ahmed[a], *Tasuku Nakajima*[b], *Takayuki Kurokawa*[b], *Md. Anamul Haque*[b,#] *and Jian Ping Gong*[b,*]

[a]Graduate School of Life Science, Hokkaido University, Sapporo 060-0810, Japan

[b]Faculty of Advanced Life Science, Hokkaido University, Sapporo 060-0810, Japan

[#]Present address: Department of Chemistry, University of Dhaka, Dhaka-1000, Bangladesh

* Corresponding author

Tel. & Fax: +81-11-706-2774, E-mail: gong@mail.sci.hokudai.ac.jp

Key words: Double network hydrogels; fracture; toughness

Abstract

Tough double network (DN) hydrogels are a kind of interpenetrating network (IPN) gels with a contrasting structure; it consists of a rigid and brittle 1st network with dilute, densely cross-linked short chains and a soft and ductile 2nd network with concentrated, loosely cross-linked long chains. In this work, we focus on how the brittle gel changes into a tough one by increasing the amount of ductile component. By comparing the molecular structures of the individual first network and second network gels, we found that the true key factor that controls the brittle-ductile transition is the density of elastically effective polymer strands of the two networks, $\nu_{e,1}$ and $\nu_{e,2}$. When $\nu_{e,2}/\nu_{e,1} < 1$, the second network fractures right after the fracture of the first network, and the gels are brittle. When $\nu_{e,2}/\nu_{e,1} > 1$, only the first network fractures. As a result, the brittle first network serves as sacrificial bonds, imparting toughness of DN gels. This result provides essential information to design tough materials based on the double network concept.

I. Introduction

Double network hydrogels or, DN gels, are regarded as one of the most robust synthetic hydrogels.[1] The tough DN gels have a very special interpenetrating network (IPN) structure. They are comprised of a rigid and brittle 1st network of densely-cross-linked short chains in dilute concentration, and a soft, stretchable 2nd network of loosely-cross-linked long chains in high concentration. The soft second network is densely packed and interpenetrated in the cage of the first network's rigid skeleton, as illustrated in **Scheme 1**. This special contrasting structure makes the DN gels extra-ordinarily tough, significantly different from conventional IPN gels. The typical tough DN gels, referred to as PAMPS/PAAm DN gels, are synthesized using poly(2-acrylamido-2-methylpropane-sulfonic acid) (PAMPS) as the first network and polyacrylamide (PAAm) as the second network.[1] The PAMPS/PAAm DN gels show high extensibility (~2,000% of original length),[1] strength (tensile fracture stress ~5 MPa)[2] and toughness (fracture energy ~1,000 J/m^2).[3,4] Later, many studies have shown that the DN concept is universal and is applicable to various species of polymeric materials, whenever the above

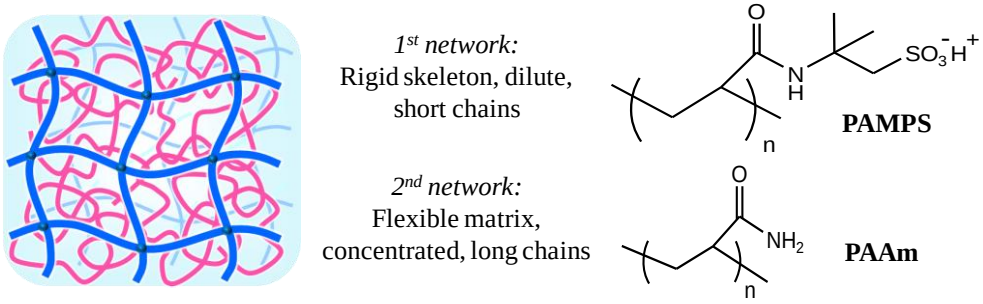

Scheme 1: Illustration of super-tough double network (DN) gels with a contrasting structure. The blue and pink lines represent the 1st and 2nd networks respectively and the filled circles indicate chemical cross-linking points. The two networks do not have internetwork chemical bond, creating a truly interpenetrating network (IPN) structure. The chemical structures of PAMPS and PAAm as first and second networks, respectively, is shown on the right.

mentioned contrasting DN structure is formed.[5-9]

Many experimental and theoretical studies have been performed to reveal the toughening mechanism of the DN gels.[10-13] These studies have revealed that the high toughness of DN gels derives from the internal fracture of the brittle network during deformation, which is observed by yielding, necking, and irreversible softening (the Mullins effect) phenomena upon tensile deformation. The internal fracture of the brittle network delocalizes the stress at the crack tip and dissipates a large amount of energy, which substantially retards the crack growth and therefore toughens the material. Previous studies[1,14] have shown that the structural essence of the tough DN gels can be summarized as follows: 1) Short first network strands and long second network strands, i.e., $N_2 >> N_1$, and 2) Low first network concentration and high second network concentration, i.e., $c_2 >> c_1$. Here N stands for the number of repeated monomeric units of polymer strands between two *chemically* cross-linked points and c indicates the molar concentration of the monomeric units of polymers.

In this study, we take notice on the latter toughening condition $c_2 >> c_1$. The sole first network is very brittle, and the DN gels containing large amount of the second network is ductile and tough. Then, how does the brittle gel change into a ductile and tough one by increasing the amount of the second ductile component c_2? In this paper, we keep the first criteria $N_2/N_1 >> 1$ satisfied and investigate the effect of the two network concentrations c_1 and c_2 on the mechanical behavior of the DN gels. For this purpose, we synthesized 3 sets of DN gels. For each set, we use a constant 1st network cross-linker density but various 2nd network concentrations. First, we prepared PAMPS single network gels with 3 different cross-linker densities. As the swelling degree of a polyelectrolyte hydrogel substantially changes with its cross-linker density, this permits us to modulate c_1 (which is roughly inverse to N_1) only by changing the cross-linker

density for preparing the 1st network. In each set of the PAMPS samples, we synthesized the second network from different AAm monomer concentration, c_{AAm} while keeping the chemical cross-linker density of the second network constant at a very small value. This permits us to keep N_2 as a large constant value, and modulate the concentration of the second network, c_2 near the transition regions. We characterized the strength and toughness of these DN gels and determined the brittle-ductile transition points against c_2. To characterize the internal fracture of these samples, we also carried out the cyclic tensile test. By comparing the tensile behavior of individual single network gels, we found that the brittle-ductile transition is strongly related to the polymer strand density ratio of the two networks, $\nu_{\mathrm{e},2}/\nu_{\mathrm{e},1}$, which indicates that the force balance between the two networks acts as the key structural parameter for this transition.

II. Experimental Section

1. Gel Synthesis

A. Materials. 2-Acrylamido-2-methylpropanesulfonic acid (AMPS) (Toa Gosei Co., Ltd.) was used as received. Acrylamide (AAm) (Junsei Chemical Co., Ltd.) was purified by recrystallizing from chloroform. Both the cross-linker *N,N'*-methylenebis(acrylamide) (MBAA) (Wako Pure Chemical Industries Ltd.) and the initiator 2-oxoglutaric acid (Wako Pure Chemical Industries Ltd.) were used as received.

B. Preparation of t-DN Gel. The first network PAMPS concentration, c_1, was varied by changing the first network cross-linker density c_{1_MBAA} and the second network concentration c_2, by changing the monomer concentration c_{AAm}. Three sets of samples were synthesized. Each set

contains the same c_{1_MBAA} but different c_{AAm}. For simplicity, we coded these DN gels as DN (*x*/*y*); where '*x*' and '*y*' are c_{1_MBAA} (mol%, with respect to the monomer concentration) and c_{AAm} (M), respectively. As has already been clarified in our previous works, conventional DN gels typically contain some internetwork bonds between the first and second networks, which are formed by copolymerization of the second network with the first network through un-reacted residual double bonds of its cross-linker.[4,15] Since truly independent DN gels (labeled *t*-DN gels) that do not contain any covalent bonds between the two networks have simpler structures than conventional DN gels, in this study we prepared *t*-DN gels for analyzing the properties of the DN gels. This time, we used the simple method to fabricate (pseudo-)*t*-DN gels. The *t*-DN gel samples were prepared using two-step sequential polymerization method with a large amount of initiator in the first network polymerization.[4] First, a glass mold was prepared by sandwiching a silicone rubber spacer (thickness varying from 1~3 mm for different experiments) between two similar glass plates. The 1st network precursor solution was prepared by dissolving 1 M of AMPS, 2, 4 or 6 mol% of MBAA as cross-linker and 1 mol% of 2-oxoglutaric acid as photo-initiator (the molar percentages are respective to the monomer concentration). The solution was then moved to an argon blanket, made oxygen-free by shaking and then poured into the pre-made glass molds. After irradiation with UV light of 365 nm wavelength from both sides for 9 hours in an argon atmosphere, the 1st network gel (PAMPS gel) was obtained. Here, the initiator concentration used was much higher than that used in the conventional DN gels which should inactivate the un-reacted residual cross-linkers of the first network. Next, these PAMPS gels were immersed and swollen in the 2nd network precursor solution which contained 0.9~2 M of AAm, 0.02 mol% of MBAA, and 0.01 mol% of 2-oxoglutaric acid for 3 days. The thickness of the as-prepared PAMPS gels was fixed at 1 mm and thicknesses of the swollen PAMPS samples in AAm

solutions are the same with those in pure water and they are tabulated in **Table S1 (Supporting information)**. The swollen PAMPS gels containing AAm monomers were then sandwiched by two glass plates, wrapped, moved to an argon blanket and again irradiated by 365 nm UV light from one side for 10 hours. In this way, the 2nd network was subsequently polymerized in the presence of the 1st network and the interpenetrating double network (DN) gels were obtained. Previous studies have implied that amount of internetwork covalent bonds in the DN gels synthesized with these compositions is too small to affect properties of them.[4] The as-prepared DN gels were then swollen in Milli-Q water for 4-5 days to remove any un-reacted monomer and then used for further tests. The sample codes and compositions used in this work are summarized in **Table 1**. The final thickness of these DN gels after swelling and the subsequent true concentrations of two networks in the DN gels along with the calculation method are shown in the supporting information section **(Supporting Figure S1)**.

For photo-polymerization purpose, we used UV lamps with an intensity of ~4 mW/cm^2 and the distance of the lamps from the sample were maintained as ~10 cm.

C. Preparation of Single Network Gels: Single network PAMPS and PAAm gels were prepared separately from the same precursor solutions of AMPS (1 M AMPS, 2, 4, 6 mol% of cross-linker and 1 mol% of initiator) and AAm (0.8~2 M AAm, 0.02 mol% cross-linker and 0.01 mol% of initiator) respectively as that for synthesizing DN gels.

Table 1. Sample codes and formulations of samples used in this study.

Sample code	**1st network**			**2nd network**		
	[Monomer], c_{AMPS} (M)	[Cross-linker], c_{1_MBAA} (mol%)	[Initiator] (mol%)	[Monomer], c_{AAm} (M)	[Cross-linker], c_{2_MBAA} (mol%)	[Initiator] (mol%)
DN (*x*/*y*)	1	2,4,6 (= ***x***)	1	0.8~2(= ***y***)	0.02	0.01
PAMPS	1	2,4,6	1	-	-	-
PAAm	-	-	-	0.8~2	0.02	0.01

*All the concentrations mentioned are the in-feed concentrations used in the precursor solutions.
** The cross-linker and initiator concentrations indicate their in-feed concentrations in mol%, with respect to the corresponding monomer concentration.

2. Characterization

A. Tensile Test. Equilibrium swollen samples (in water) were used for tensile tests of DN gels whereas as-prepared samples were used for sole PAAm gels. For sole PAMPS gels, both swollen and as-prepared ones were used. All the tensile tests were carried out at 25°C in air environment and pre-cut dumbbell shaped gel samples (**Figure 1a**) standardized as the JIS-K6251-7 size (length of the thinner portion, *L*: 12mm, width of the thinner portion, *b*: 2mm, thickness, *w*: 1.5~3 mm) were used. A commercial tensile tester Instron 5965 (Instron Co.) equipped with an advanced video extensometer (AVE) was applied for measuring tensile stress-strain (SS) curves of the samples at a fixed tensile velocity of 100 mm/min. For DN gels and PAMPS gels, the accurate strain was measured by real-time observation of the distance between two white spots marked on the thin portion of the sample with the video extensometer. Only nominal strain was determined in the case of sole PAAm gels, as their high stretchability exceeded the view range of the video extensometer. The fracture stress, σ_f (Pa), was obtained

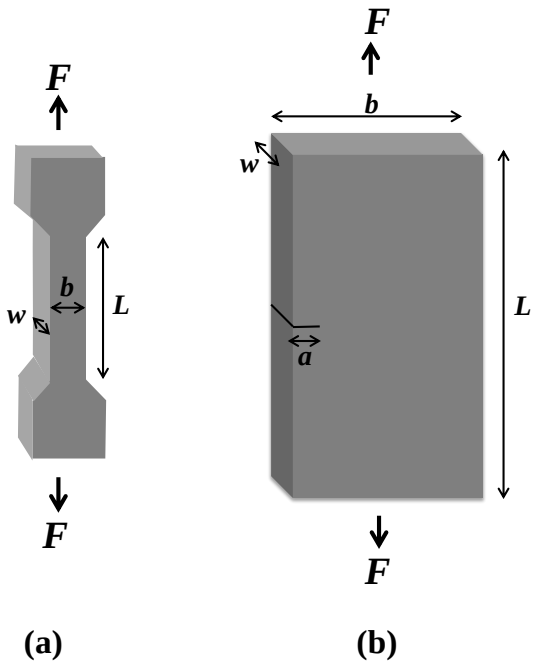

Figure 1: Illustration of different shapes of gel samples used for the characterization: **(a)** dumbbell-shaped sample for tensile/cyclic tensile test and **(b)** bar-shaped sample with a pre-notch for tearing test .

from the nominal stress value at the fracture point. The work of extension to fracture, W_{ext} (J/m^3), which is an indication of toughness of materials, was measured from the area under the SS curve until fracture point. The Young's modulus, *E*, was determined as the slope of nominal stress-strain curves between the strain range of 0.02~0.2. Each data was the average of 4 measurements, and the error bars were obtained from their standard deviations.

B. Tensile Test with Pre-notched Samples. Tensile test was performed on pre-notched bar-shaped samples (illustration in **Figure 1b**) (length, *L*= 30 mm, width, *b*= 10 mm, thickness, *w*= 4~5 mm, initial notch length, *a*= 1.5 mm) with the tensile tester Instron 5965 (Instron Co.) at 25°C in the air. One end of the bar-shaped sample was fixed with clamp and the other end was

pulled at a constant velocity of 100 mm/min. Crack propagation in mode I (tensile mode of crack opening) was observed as a result of applying force F, and the stress intensity factor, K_I, ahead of the crack tip was calculated from the following equation,[16]

$$K_I = \sigma\sqrt{a}(1.99 - 0.41x + 18.7x^2 - 38.5x^3 + 53.9x^4) \qquad (1)$$

where, σ is the stress applied (σ=$F/w(b-a)$), x is the ratio a/b. The tearing energy, T (J/m^2), defined as the energy required to fracture a unit surface area in the sample, was calculated as,

$$T = K_{Ic}^2(1 - v^2)/E \qquad (2)$$

where, K_{Ic} is the critical stress intensity factor for crack propagation, and it was measured from the critical stress at which the pre-notched crack started to propagate, E is the Young's modulus and v is the Poisson's ratio of the soft material (gel). In this paper, we considered the value of v as 0.5. The fracture energy T thus defined is two times of the energy required to create a unit fractured surface.[16] Each data was the average of 4 measurements, and the error bars indicate standard deviations.

C. Cyclic Tensile Test. For cyclic tensile test, dumbbell shaped samples standardized as JIS-K6251-7 size, same as those for tensile test **(Figure 1a)**, were used and Instron 5965 (Instron Co.) tensile tester equipped with AVE was applied to record the successive cyclic tensile stress-strain curves. All the tests were carried out in the air environment at 25°C. First, the sample was loaded up to a pre-assigned strain, ε_{max} and then unloaded until reaching at a strain zero. Then, they were immediately loaded again up to a pre-fixed higher strain and then unloaded. In this way, the same sample was loaded and unloaded up to gradually increasing strain values until

fracture. As in the case of DN gels, a successive loading curve completely overlaps with the unloading curve of the previous cycle,[17,18] we consider only the loading curves instead of the unloading curves for simplicity. The dissipated energy, $U_{hys}(\varepsilon_{max})$ (J/m^3), defined as the area enclosed by the first and second loading curves up to the strain ε_{max} of the first loading, was calculated as

$$U_{hys}(\varepsilon_{max}) = \int_0^{\varepsilon_{max}} \sigma_1 \, d\varepsilon - \int_0^{\varepsilon_{max}} \sigma_2 \, d\varepsilon \qquad (3)$$

where, σ_1 and σ_2 are the nominal stress values for the first and second loading curves, respectively.

III. Results & Discussion

Tensile Behavior of the DN Gels. The tensile stress-strain (SS) curves of DN (2/*y*), DN (4/*y*) and DN (6/*y*) gels are shown in **Figure 2(a-c)**, respectively. When the 2nd network monomer concentration, *y* is enough high, the DN gels show high fracture stress and fracture strain, and also, the significant 'yielding' phenomenon, which greatly contributes to the excellent toughness of DN gels.[10-13] These robust DN gels which show this exclusive yielding phenomenon are defined as '*ductile*' DN gels. On the other hand, when *y* is reduced while keeping the same 1st network, the fracture stress and strain of the DN gels suddenly decreases after certain points. For example, in the case of DN (4/*y*), fracture stress remarkably decreases when *y* is slightly decreased from 1.1 to 1. Such DN gels undergo fracture much earlier before yielding appears. Thus, these weak DN gels which do not show yield point are defined as '*brittle*' DN gels, and such sudden transformation in fracture parameters has been termed here as '*brittle-ductile transition*'.

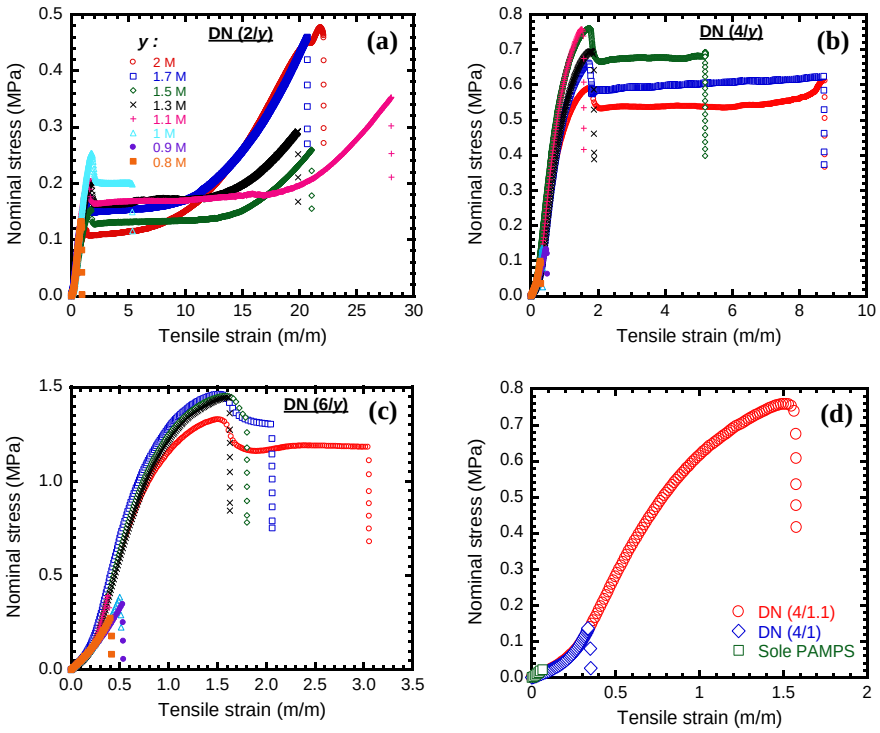

Figure 2: The tensile stress-strain curves of **(a)** DN (2/*y*); **(b)** DN (4/*y*); **(c)** DN (6/*y*) gels and **(d)** sole PAMPS, DN (4/1) and DN (4/1.1) gels, where '*y*' is the AAm monomer concentration in feed. The symbols and colors for different compositions in (b), (c) are the same as in (a). Tensile stretching rate was 100 mm/min. Compared to the brittle ones, the other compositions show much higher toughness.

When we compared the tensile SS curves of DN (4/1) (brittle) and DN (4/1.1) (ductile) gels with the sole PAMPS gel (**Figure 2d**), it is clearly seen from the fracture point that brittle DN gel is only slightly stronger than the sole PAMPS gel which is extremely brittle. The critical *y* for obtaining ductile DN gels y_c were determined as 1.0, 1.1, and 1.3 M for DN (2/*y*), (4/*y*), and (6/*y*) gels, respectively. We find that as *x* (1st network cross-linker concentration) increases, which correspond to an increase of PAMPS concentration, y_c also increases. This phenomenon suggests that the brittle-ductile transition is not only governed by one network, rather it is governed by the two networks.

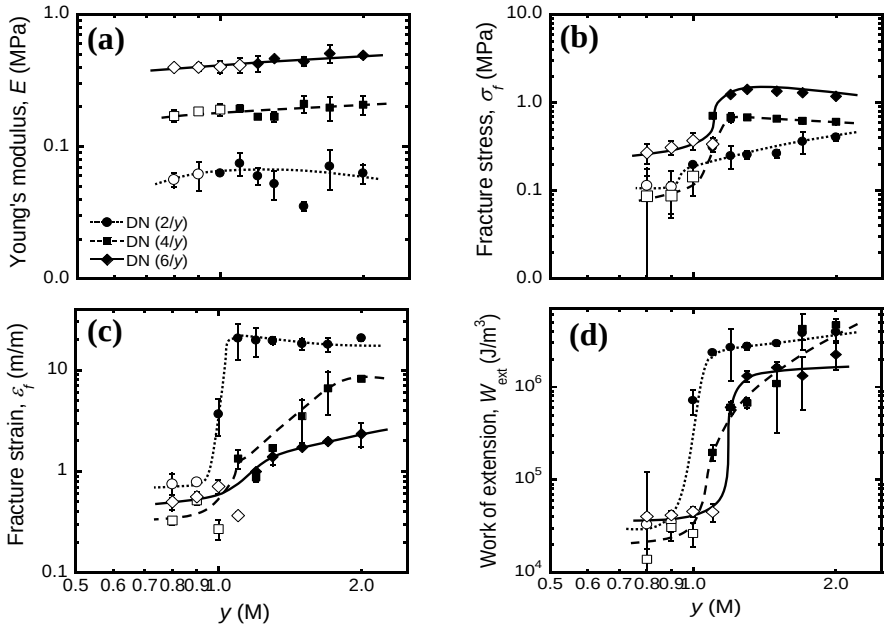

Figure 3: The mechanical toughness characterizing parameters **(a)** Young's modulus, E **(b)** fracture stress, σ_f **(c)** fracture strain, ε_f, and **(d)** work of extension, W_{ext} against AAm monomer concentration in feed, y in DN (2/y), DN (4/y) and DN (6/y) gels. The closed and open symbols indicate ductile and brittle samples respectively and the symbols in (b)-(d) are the same as in (a). In both cases, brittle samples show much smaller values of the parameters showing very low toughness.

Figure 3 shows the Young's modulus (E), fracture stress (σ_f), fracture strain (ε_f), and work of extension (W_{ext}) against the AAm in feed concentration, y (**Figure 3**). For a constant set of the PAMPS network, the moduli of the DN gels change very slightly with changing y (**Figure 3a**). It means that the brittle-ductile transition does not affect the moduli of DN gels. On the other hand, the other parameters were remarkably changed in response to brittle-ductile transition. In terms of the fracture stress, the brittle to ductile transition becomes more abrupt for the sample with high cross-linker density of PAMPS (DN (6/y)) (**Figure 3b**). In contrast, in terms of fracture strain, we observed an opposite trend (**Figure 3c**). As a result, the work of extension shows an abrupt transition with y for all the 3 sets of samples (**Figure 3d**).

Tensile Behavior of Pre-notched DN Gel Samples. To characterize the toughness, we used uniaxial stretching to pre-notched bar-shaped DN gel samples.[19] We calculated the tearing energy of both ductile and brittle DN gel samples by estimating the critical stress intensity factor

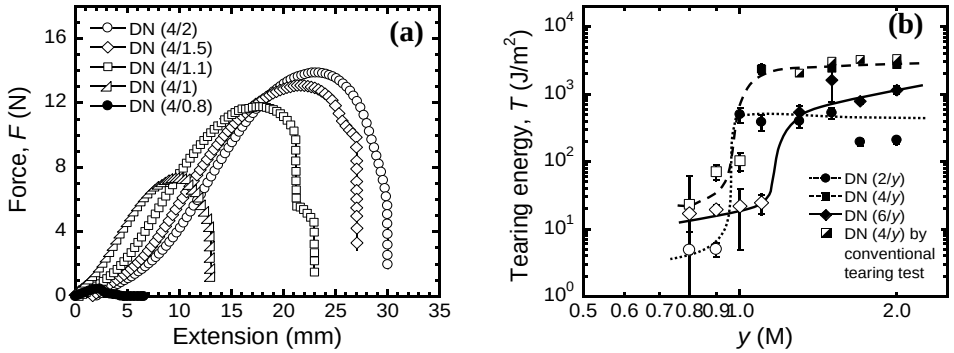

Figure 4: (a) The typical load vs. extension curves for brittle DN (4/0.8), (4/1) and ductile DN (4/1.1), (4/1.5) and (4/2) gels and **(b)** calculated tearing energy, *T* values for DN (2/*y*), (4/*y*) and (6/*y*) gels from tearing test. The brittle DN gels (open symbols in (b)) require much reduced force and energy for crack propagation indicating low crack propagation resistance and hence, very small toughness.

for crack propagation (K_{Ic}).[20,21] **Figure 4a** represents the resulting force vs. extension curves for brittle DN (4/0.8), (4/1) and several ductile DN gel samples. It is obvious from this figure that the applied force at which the pre-notch is converted to a running crack is high in all the ductile DN samples; those are, DN (4/1.1), (4/1.5) and (4/2) compositions; but has a much lower value in the case of the brittle compositions DN (4/0.8) and (4/1). That means, a much smaller force is required to initiate crack propagation in the brittle DN gel sample, in contrast to the ductile ones.

The tearing energy (*T*) calculated using Eq. 1 and Eq. 2 for different brittle and ductile compositions is shown in **Figure 4b**. An abrupt increase in the tearing energy *T* is also observed

at critical y_c values, in consistence with the tensile results in **Figure 3d**. Note that tearing test of a trouser-shaped DN sample with pre-crack[22,23] has been used to determine gel toughness in our previous studies.[3,24] This time we could not apply this method for the brittle DN gels because they undergo fracture at the bending point of samples due to their brittle nature. In addition, we have confirmed that the tearing energy values of the ductile DN gels determined by the present method are in agreement with those measured from the tearing test using conventional trouser-shaped samples[19,20], as shown in **Figure 4b**.

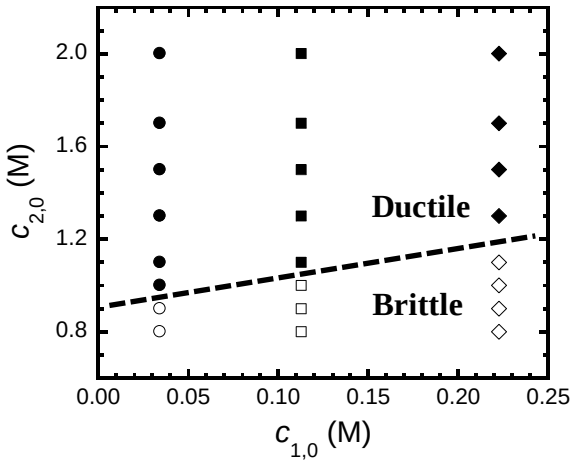

Figure 5: Composition-dependent brittle-ductile phase diagram for different sets of DN gels used in our work. $c_{1,0}$ and $c_{2,0}$ represent the true concentrations of the 1st and 2nd networks in the as-prepared DN gels, respectively. The circles (●), squares (■) and diamond (♦) shapes indicate the samples DN (2/*y*), DN (4/*y*), and DN (6/*y*), respectively; whereas the filled and open symbols indicate ductile and brittle samples respectively, identified from tensile and tearing test results of their swollen forms.

From the above results, we can construct a mechanical phase diagram in the space of concentrations of the first and second networks (**Figure 5**). As the entanglement between the two networks depends on the concentrations of the two components at which the IPN structure is

formed, we adopt the 1st network and 2nd network concentrations, $c_{1,0}$ and $c_{2,0}$, respectively, of the as-prepared IPN samples. Here $c_{1,0}$ was estimated from the thicknesses of the PAMPS gels in their as-prepared and swollen states and $c_{2,0}$ was estimated as $c_{2,0}=c_{AAm}$, assuming 100% polymerization efficiency of the precursor monomers[25] (**Supporting Information**). **Figure 5** shows that the critical $c_{2,0}$ for transition only slightly increases with $c_{1,0}$. The physical meaning of this exclusive phenomenon will be discussed later.

Mechanical Hysteresis Behavior. As has been revealed by the previous studies of our group, the DN gels are toughened by the internal fracture mechanism. This internal fracture of PAMPS remarkably increases the energy for crack growth and delocalizes the stress at the crack tip. As a result, the crack propagation in DN gels is retarded.[26,27] To relate the brittle-ductile transition to

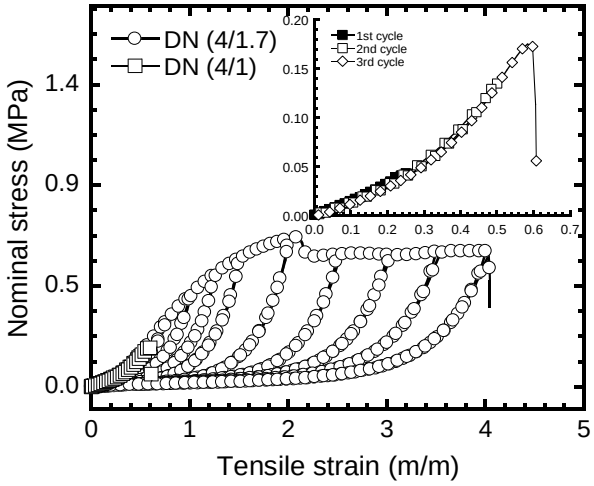

Figure 6: Comparative successive loading curves of brittle DN (4/1) and ductile DN (4/1.7) gels obtained from the cyclic tensile test after applying increasing amount of strain (until fracture). The inset figure provides an enlarged view of the curves of DN (4/1) including different loading cycles which overlap with each other showing almost no hysteresis till sample failure.

the structure change of the PAMPS network, we further characterized the internal fracture behavior of PAMPS by measuring the hysteresis of the repeated cyclic tensile elongation. The cyclic stress-strain (c-SS) curves of ductile DN (4/1.7) and brittle DN (4/1) gels are shown in **Figure 6**. The inset figure enlarges the c-SS curves for the brittle sample. For the ductile samples, they show very large amount of hysteresis (i.e. energy dissipation) above a certain strain, and the hysteresis increases with the applied strain until sample breakage. On the contrary, the brittle sample breaks at a very small strain and exhibits almost no hysteresis until breakage. Subsequently, we calculated the amount of dissipated energy from the area of the c-SS curves as a result of applying different amount of strain (**Figure 7a**) for the brittle (4/1), moderately tough (4/1.5) and the toughest (4/2) DN gels. DN (4/1.5) and DN (4/2) hydrogels initially exhibit very

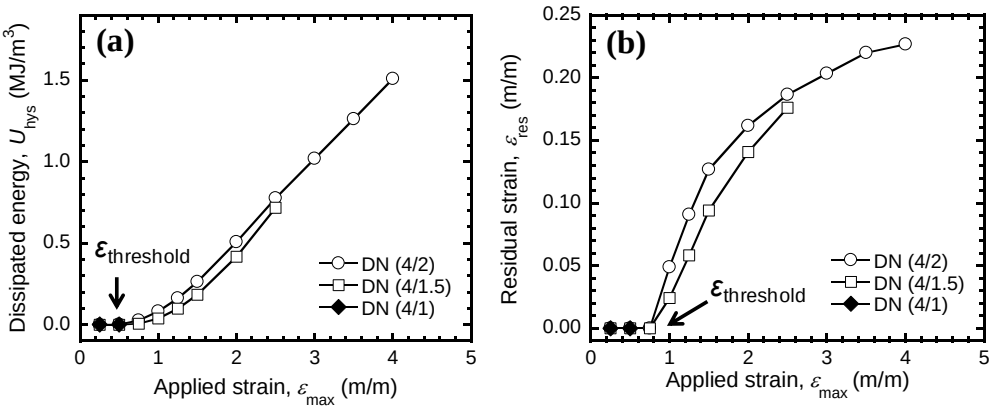

Figure 7: The trend of increasing **(a)** dissipated energy, U_{hys} and **(b)** residual strain, ε_{res} as function of the maximum applied strain, ε_{max} for brittle DN (4/1), moderately tough (4/1.5) and toughest (4/2) gels. The brittle gel fractures before reaching $\varepsilon_{threshold}$, without showing U_{hys} and ε_{res}.

little energy dissipation up to a certain strain (we assign it as the 'threshold strain for energy dissipation', $\varepsilon_{threshold}$) and then the energy dissipation increases linearly with increasing strain, in consistence with our recent works.[18] On the other hand, the brittle DN (4/1) shows almost no energy dissipation and fractures immediately once it reaches the $\varepsilon_{threshold}$. Apparently, the $\varepsilon_{threshold}$ is the point at which the internal fracture of the 1st network starts. For the brittle sample, this starting of the internal fracture leads to propagation of the micro crack and brings sudden global failure of both the PAMPS and PAAm networks. On the other hand, for the ductile sample, the propagation of the 1st network is stopped by the PAAm network. In the latter process, the stress is transferred to a far region behind the crack, which leads to wide-scale internal fracture of the PAMPS network while keeping the structural integrity of the gels.

The internal structural change of materials usually brings about residual strain after deformation. We also investigated the residual strain for different cycles from the c-SS curves for the above-mentioned three compositions (**Figure 7b**). The brittle DN (4/1) sample that shows elastic behavior exhibits no residual strain until fracture at the $\varepsilon_{threshold}$. On the other hand, the ductile samples, DN (4/1.5) and DN (4/2), do exhibit residual strain above the threshold strain ($\varepsilon_{threshold}$), in consistent with the internal fracture of the 1st network. The residual strains, although very small in comparison with the large strains the samples experienced, go through a continuous increase with increasing applied strain. Considering the incompressible nature of gels (Poisson's ratio ν = 0.5), these residual strains should bring about a decrease in the cross sectional area of the sample, which can be attributed to the anisotropic fracture of the PAMPS network.[18]

From above results, features of the brittle and the ductile DN gels can be distinguished as follows; the former are brittle, weak, and fracture before catastrophic internal fracture of the 1st

network whereas the latter are ductile, strong, and fracture after wide-range internal fracture of the 1st network. Therefore, brittle-ductile transition also can be defined by presence or absence of internal fracture.

Mechanical Balance of Two Networks. Then, the question is what determines the occurrence of effective internal fracture? As DN gels consist of two individual networks, it should be governed by the mechanical balance of the two networks. Ideally, this mechanical balance is related to the strength of the two networks, which is determined by their number density of elastically effective polymer strands, $\nu_{e,1}$ and $\nu_{e,2}$. We assume that at the brittle-ductile transition point, $\nu_{e,1}$ and $\nu_{e,2}$ are equal. To confirm this assumption, first, we discuss on $\nu_{e,1}$ and $\nu_{e,2}$ in the as-prepared DN gels.

The $\nu_{e,1}$ of the first network is equal to that of the sole PAMPS gel in swollen state, $\nu_{e,1}^{s}$. For the $\nu_{e,2}$ of the second soft network in DN gels, we should consider three contributions: chemical cross-linking, trapped entanglement between second network polymer chains, and entanglement of second network polymer chains to the first network. The contribution of internetwork entanglement is also evident in **Figure 3c**, where we found that ε_f of DN gels decreases with increasing first network cross-linker density *x*, indicating that the enhanced entanglement of the second network with the first network decreases the extensibility of PAAm chains. The latter two contributions of physical entanglements are predominant in measuring $\nu_{e,2}$ since we used extremely low amount of chemical cross-linker (1 mole of cross-linker for every 5000 moles of monomer) for 2nd network preparation. Assuming that the polymerization of AAm monomers in

the presence of PAMPS network is the same as that of sole PAAm gel,[17] the sum of the first and second contributions to $\nu_{e,2}$ can be estimated from the sole PAAm gels $\nu_{e,2}^{s}$.

Therefore, we investigated the tensile behaviors of individual single network PAMPS gels in swollen state and PAAm gels in as-prepared state, with the same formulation as that of as-prepared DN gels. As shown in **Figure 8**, PAMPS gels are rigid and brittle; thus they fracture at very small strains (nominal fracture strain, ε_f <0.35). On the other hand, PAAm gels are soft and

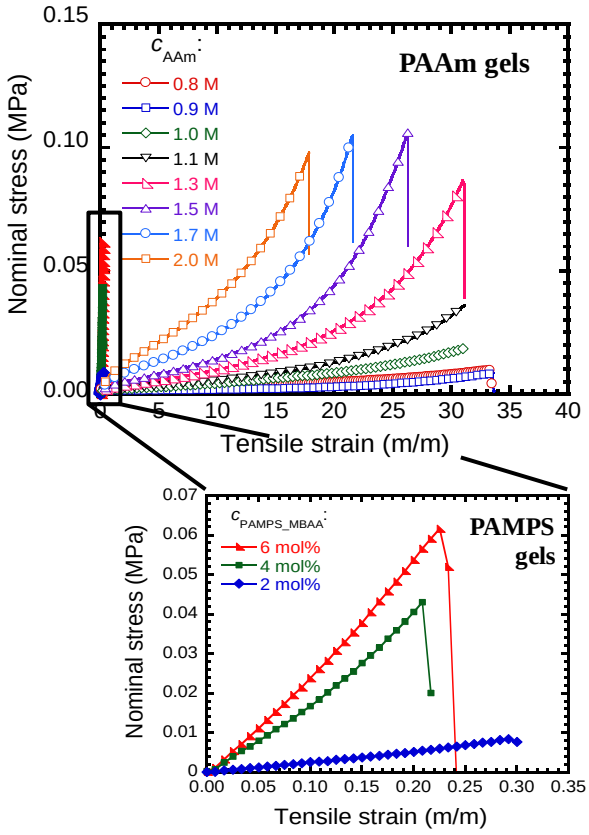

Figure 8: The tensile SS curves of sole PAMPS and PAAm gels having the same concentrations as in their corresponding DN gels. Only a portion of data is shown for a clearer view. Tensile SS curves of sole PAMPS gels are magnified in to a separate figure in the bottom-right for better visibility.

ductile, showing large fracture strains (ε_f =15-35). The $\nu^s_{e,1}$ and $\nu^s_{e,2}$, which are number densities of elastically effective polymer strands of each single network, can be estimated from the Young's moduli of the gels.

Rubber elasticity theories have shown that the number density of elastic strands in Gaussian conformation is related to the Young's moduli of the gels by Eq.4.

$$E = 3\nu_e RT \quad (4)$$

Where E is Young's modulus, R is gas constant, and T is temperature. Since the polymer strands in the neutral gel are in Gaussian conformation, we simply estimated $\nu^s_{e,2}$ from the as-prepared PAAm gels by equation 4 (**Table S2, supporting information**). As the polymer strands of swollen PAMPS gel are not in Gaussian conformation, we could not estimate $\nu^s_{e,1}$ directly from its modulus. Instead, we first estimated the strand density of as-prepared PAMPS gels using 2, 4 and 6 mol% c_{PAMPS_MBAA} and then, we estimated $\nu^s_{e,1}$ using the following equation,

$$\nu^s_{e,1} = \frac{E_0}{3RT}\left(\frac{t^0_{PAMPS}}{t_{PAMPS}}\right)^3 \quad (5)$$

Where, E_0 is the Young's modulus of the as-prepared PAMPS gels, $t_{PAMPS}{}^0$ and t_{PAMPS} are the thicknesses of as-prepared and equilibrium swollen PAMPS gels respectively (**Table S1, supporting information**).

To elucidate the effect of the network structure on the transition, we first plotted the transition diagram in $\nu^s_{e,1}$- $\nu^s_{e,2}$ space, without incorporating the internetwork entanglement effect. Except at very small $\nu^s_{e,1}$, the critical $\nu_{e,2}{}^s$ for transition is not equal to, but lower than $\nu^s_{e,1}$ **(Figure 9a)**. This fact suggests that the third contribution (internetwork entanglement) becomes

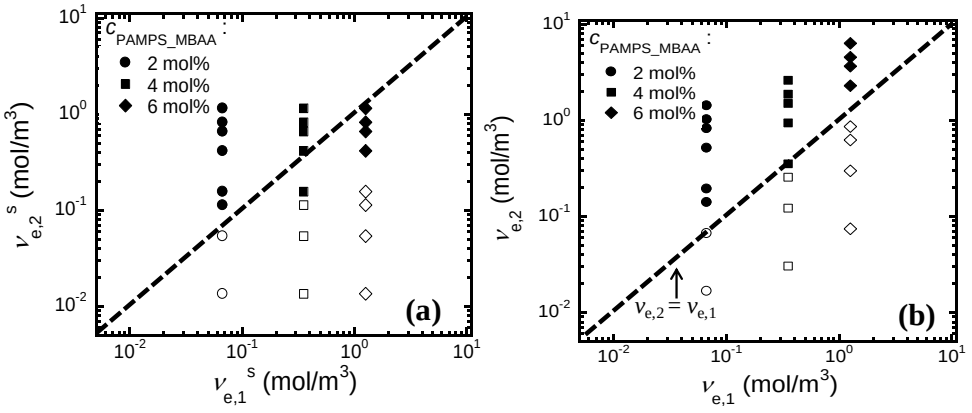

Figure 9: Brittle-ductile phase diagrams in polymer strand density space. **(a)** $\nu_{e,2}^{s}$ vs. $\nu_{e,1}^{s}$, without considering the internetwork entanglement; **(b)** $\nu_{e,2}$ vs. $\nu_{e,1}$, after including the correction term for inter-network entanglement for the second network (3.6 $\nu_{e,1}^{s}\nu_{e,2}^{s}$). In (b), all the ductile points (filled symbols) are located above the line of $\nu_{e,2} = \nu_{e,1}$, whereas brittle points (open symbols) fall below that line.

important with the increase of $\nu_{e,1}^{s}$ for the transition of DN gels. The 3rd contribution from the entanglement between the two networks should depend on the chain density of both, and the overall 2nd network strand density thus can be expressed as,

$$\nu_{e,2} = \nu_{e,2}^{s} + k\nu_{e,1}^{s}\nu_{e,2}^{s} \qquad (6)$$

Where $\nu_{e,1}^{s}$, $\nu_{e,2}^{s}$ values are determined from sole networks and k is an unknown constant having a unit of m^3/mol. On the other hand, we can assume $\nu_{e,1} = \nu_{e,1}^{s}$, since the 1st network is much more rigid than the 2nd network, and hence it's deformation will not be influenced by the entanglement with the 2nd network. Accordingly, we plotted $\nu_{e,2}$ vs. $\nu_{e,1}$ (=$\nu_{e,1}^{s}$) as shown in **Figure 9b** and found that by using k = 3.6 m^3/mol, the brittle and ductile data points fall in two different regions separated by a border line $\nu_{e,1} = \nu_{e,2}$.

This result suggests that the brittle-ductile transition of DN gels is governed by the ratio of the polymer strand densities of the two networks, which is also equivalent to their strength ratio, whereupon the internetwork entanglement plays a very important role. When the PAAm network has higher chain density than PAMPS ($\nu_{e,2}/\nu_{e,1}$>1), DN gels become ductile and tough. Conversely, when the chain density of PAAm is lower than that of PAMPS ($\nu_{e,2}/\nu_{e,1}$<1), the DN gels are weak and brittle. Thus, we conclude that $\nu_{e,1}^{s} = \nu_{e,2}^{s}$ is the critical condition to determine the brittle-ductile transition.

Two-Spring Model for Brittle-Ductile Transition. The previous experiments and analyses clearly show that the essence of the brittle-ductile transition is the mechanical balance of the two networks. Based on this result, we try to illustrate this brittle-ductile transition in double network gels adopting a two-spring model as shown in **Figure 10**. The blue and red springs signify the state of the 1st and 2nd network strands in any tiny zone of DN gel, respectively when tensile stress, σ is applied on it. For both brittle and ductile gels, the stiff and short PAMPS strands that are in highly extended state fracture first around the threshold strain, $\varepsilon_{threshold}$. Once this happens, the applied force is transferred to the soft and long PAAm strands that are in coiled state, making them locally stretched. Now, if $\nu_{e,2} > \nu_{e,1}$, these PAAm strands can sustain the force transferred. As the two networks are strongly entangled with each other, in the first case, the stretched PAAm strands also transfer force to PAMPS strands and induce their fracture, which leads to wide-range internal fracture of PAMPS, *i.e.* high toughness of DN gels. Oppositely, if $\nu_{e,2} < \nu_{e,1}$, these PAAm strands cannot sustain the stress and fracture right after the fracture of PAMPS strands. As a result, global sample failure occurs without large energy dissipation.

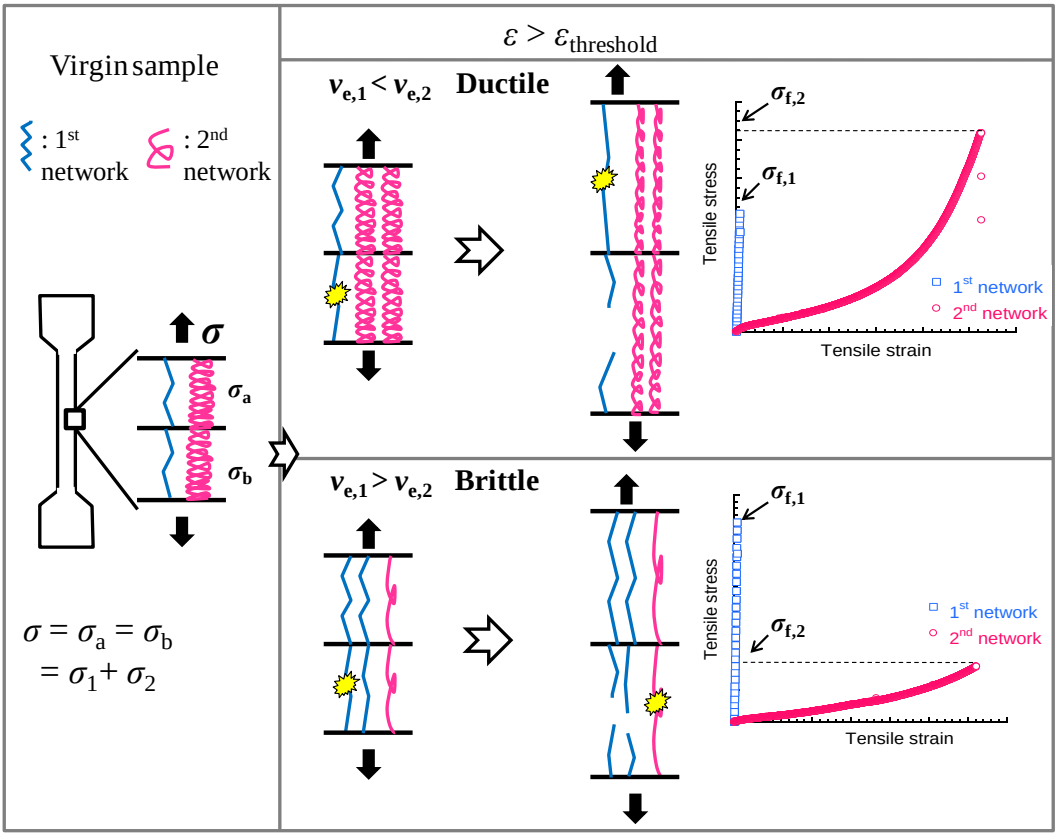

Figure 10: Illustration of the tensile stretching of ductile and brittle DN gels using two springs as model. With stretching, the ductile DN gel (where the effective chain number density of the 2nd network is higher than that of the 1st network) experiences internal damage of the 1st network, while the brittle DN gel (where chain density of the 1st network is higher than that of the 2nd network) undergoes simultaneous fracture of the two networks, which leads to sample failure.

IV. Conclusions

The composition-dependent brittle-ductile transition of DN gels is determined by the mechanical balance of the two networks, in which the effective polymer strand density ratio of the two networks, $\nu_{e,2}/\nu_{e,1}$, serves as the key parameter. When the brittle first network has less strand density than the ductile second network ($\nu_{e,2}/\nu_{e,1}>1$), the DN gels become tough. Conversely,

when the brittle network has higher chain density than the ductile network ($\nu_{e,2}/\nu_{e,1}$<1), the DN gels become brittle. As the brittle network is comprised of short and extended chains, it always ruptures first, by which the stress is transferred to the ductile network. In the case of $\nu_{e,2}/\nu_{e,1}$ >1, the propagation of the micro-crack in the brittle network is stopped by the ductile network, and the latter transfer the stress to a wide region to cause further internal damage of the brittle network. As a result, the brittle network dissipates large amount of energy working as sacrificial bonds and the toughness of the gels is abruptly enhanced. On the other hand, in the case of $\nu_{e,2}/\nu_{e,1}$<1, the ductile network cannot sustain the stress transferred from the brittle network, and it ruptures simultaneously. As a result, the crack propagates catastrophically which leads to an immediate grand failure of the sample to show brittleness. This immediate fracture of PAAm network just after that of PAMPS prevents the internal fracture of the 1st network, thus leads to negligible energy dissipation by brittle samples. Accordingly, a mechanical definition of the DN hydrogels is different from the IPN hydrogels in the sense that DN hydrogels have internal fracture before failure. Except for very low $\nu_{e,1}$ of the first network, $\nu_{e,2}$ of the second network is dominated by internetwork entanglement. The criteria $\nu_{e,2}/\nu_{e,1}$>1 for obtaining tough DN gels is universal and should be used as the key parameter to design tough materials based on the double network concept.

Acknowledgement

This work was supported by a Grant-in-Aid for Scientific Research (S) (No. 124225006) from Japan Society for the Promotion of Science (JSPS).

References

1. Gong, J. P.; Katsuyama, Y.; Kurokawa, T.; Osada, Y. *Adv. Mater.* **2003**, *15*, 1155.
2. Kawauchi, Y.; Tanaka, Y.; Furukawa, H.; Kurokawa, T.; Nakajima, T.; Osada Y.; Gong, J. P. *J. Phys. Conf. Ser.* **2009**, *184*, 012016.
3. Tanaka, Y.; Kuwabara, R.; Na, Y. –H.; Kurokawa, T.; Gong, J. P.; Osada, Y. *J. Phys. Chem. B.* **2005**, *109*, 11559.
4. Nakajima, T.; Furukawa, H.; Tanaka, Y.; Kurokawa, T.; Osada Y.; Gong, J. P. *Macromolecules* **2009**, *42*, 2184.
5. Hu, J.; Kurokawa, T.; Hiwatashi, K.; Nakajima, T.; Wu, Z. L.; Liang S.; Gong, J. P. *Macromolecules* **2012**, *45*, 5218.
6. Nakajima, T.; Sato, H.; Zhao, Y.; Kawahara, S.; Kurokawa, T.; Sugahara, K. Gong, J. P. *Adv. Funct. Mater.* **2012**, *22*, 4426.
7. Suekama, T. C.; Hu, J.; Kurokawa, T.; Gong, J. P., Gehrke, S. H. *ACS Macro Lett.* **2013**, *2*, 137.
8. Nakajima, T.; Fukuda, Y.; Kurokawa, T.; Sakai, T.; Chung, U.; Gong, J. P. *ACS Macro Lett*. **2013**, *2*, 518.
9. Haiyan, Y.; Akasaki, T.; Sun, T. L.; Nakajima, T.; Kurokawa, T.; Nonoyama, T.; Taira, T.; Saruwatari, Y.; Gong, J. P. *J. Mater. Chem. B* **2013**, *1*, 3685.
10. Na, Y. –H.; Tanaka, Y.; Kawauchi, Y.; Furukawa, H.; Sumiyoshi, T.; Gong, J. P.; Osada, Y. *Macromolecules* **2006**, *39*, 4641.
11. Webber, R.; Creton, C.; Brown, H. R.; Gong, J. P. *Macromolecules* **2007**, *40*, 2917.
12. Brown, H. R. *Macromolecules* **2007**, *40*, 3815.
13. Tanaka, Y. *Europhys. Lett*. **2007**, *78*, 56005.

14. Na, Y. –H.; Kurokawa, T.; Katsuyama, Y.; Tsukeshiba, H.; Gong, J. P.; Osada, Y.; Okabe, S.; Karino, T.; Shibayama, M. *Macromolecules* **2004**, *37*, 5370.

15. Tominaga, T.; Tirumala, V. R.; Lin, E. K.; Gong, J. P.; Wu, W. –L. *J. Phys. Chem. B* **2007**, *112*, 3903.

16. Hertzberg, R. In *Deformation and Fracture Mechanics of Engineering Materials*, John Wiley and Sons: New York, 1996; p 757.

17. Tsukeshiba, H.; Huang, M.; Na, Y. –H.; Kurokawa, T.; Gong, J. P.; Osada, Y. *J. Phys. Chem. B.* **2005**, *109*, 11559.

18. Nakajima, T.; Kurokawa, T.; Ahmed, S.; Wu, W. –L.; Gong, J. P. *Soft Matter* **2013**, *9*, 1955.

19. Lin, W. –C.; Fan, W.; Marcellan, A.; Hourdet, D.; Costantino, C. *Macromolecules* **2010**, *43*, 2554.

20. Evans, A. G. In *Fracture mechanics of ceramics*, Plenum, New York, 1974; Vol. 1, p 17.

21. Zarzycki, J. *J. Non-Cryst. Solids* **1988**, *100*, 359.

22. Rivlin, R. S.;Thomas, A. G. *J. Polym. Sci.***1953**,*10*, 291.

23. Greensmith, H. W.;Thomas, A. G. *J. Polym. Sci*.**1955**,*18***,** 189.

24. Furukawa, H.; Kuwabara, R.; Tanaka, Y.; Kurokawa, T.; Na, Y. –H.; Osada, Y.; Gong, J. P. *Macromolecules* **2008**, *41*, 7173.

25. Kii, A.; Xu, J.; Gong, J. P.; Osada, Y.; Zhang, X. *J. Phys. Chem. B* **2001**, *105*, 4565.

26. Tanaka, Y.; Kawauchi, Y.; Kurokawa, T.; Furukawa, H.; Okajima, T.; Gong, J. P. *Macromol. Rapid Commun*. **2008**, *29*, 1514.

27. Yu, Q. M.; Tanaka, Y.; Furukawa, H.; Kurokawa, T.; Gong, J. P. *Macromolecules* **2009**, *42*, 3852.

For Table of Contents (TOC) use only

Brittle-Ductile Transition of Double Network Hydrogels: Mechanical Balance of Two Networks as the Key Factor
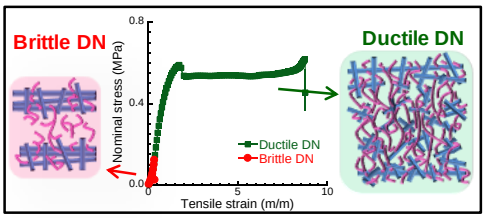
Saika Ahmed, Tasuku Nakajima, Takayuki Kurokawa, Md. Anamul Haque, and Jian Ping Gong